Received: 30 May 2021 | Accepted: 7 December 2021

DOI: 10.1002/bab.2300

ORIGINAL ARTICLE

WILEY

Biosensing epidemic and pandemic respiratory viruses: Internet of Things with Gaussian noise channel algorithmic model

Subash C.B. Gopinath[1,2,3] | **Zool H. Ismail**[4] | **Kazuma Sekiguchi**[5]

[1] Institute of Nano Electronic Engineering, Universiti Malaysia Perlis (UniMAP), Kangar, Perlis 01000, Malaysia

[2] Faculty of Chemical Engineering Technology, Universiti Malaysia Perlis (UniMAP), Arau, Perlis 02600, Malaysia

[3] Centre of Excellence for Nanobiotechnology and Nanomedicine (CoExNano), Faculty of applied Sciences, AIMST University, Semeling, Kedah 08100, Malaysia

[4] Centre for Artificial Intelligence and Robotics, Universiti Teknologi Malaysia (UTM), Jalan Sultan Yahya Petra, Kuala Lumpur 51400, Malaysia

[5] Advanced Control Systems Laboratory, Department of Mechanical Systems Engineering, Tokyo City University (TCU), Tamazutsumi Setagaya-ku, Tokyo 158-8557, Japan

Correspondence
Subash C.B. Gopinath, Faculty of Chemical Engineering Technology, Universiti Malaysia Perlis, Perlis, Malaysia.
Email: subash@unimap.edu.my

Abstract

The current world condition is dire due to epidemics and pandemics as a result of novel viruses, such as influenza and the coronavirus, causing acute respiratory syndrome. To overcome these critical situations, the current research seeks to generate a common surveillance system with the assistance of a controlled Internet of Things operated under a Gaussian noise channel. To create the model system, a study with an analysis of H1N1 influenza virus determination on an interdigitated electrode (IDE) sensor was validated by current–volt measurements. The preliminary data were generated using hemagglutinin as the target against gold-conjugated aptamer/antibody as the probe, with the transmission pattern showing consistency with the Gaussian noise channel algorithm. A good fit with the algorithmic values was found, displaying a similar pattern to that output from the IDE, indicating reliability. This study can be a model for the surveillance of varied pathogens, including the emergence and reemergence of novel strains.

KEYWORDS

acute respiratory syndrome, algorithm, biosensor, influenza virus, remote digital monitoring

1 | INTRODUCTION

Currently, it is critical to overcome issues generated by novel respiratory pandemic viruses, which cause acute respiratory syndrome. The present condition is not new; similar situations have occurred in the past decades as a result of several respiratory viral complications, such as swine flu, bird flu, severe acute respiratory syndrome, Middle East respiratory syndrome, and the current pandemic with COVID-19. Among these, influenza viruses have caused several epidemics and pandemics by emerging and reemerging as new strains worldwide with seasonal variations. Influenza viruses are classified into A, B, and C, among which the first two influenza types are predominant and type C is minor.[1–4] Influenza A is more severe than influenza B, and several subtypes have arisen from influenza-type A, such as H1N1, H2N2, H3N2, H5N1,

Abbreviations: COVID, Coronavirus disease; fM, Femtomolar; GNP, Gold nanoparticle; HA, hemagglutinin; IDE, Interdigitated electrode; IoT, Internet of Things; KF, Kalman filter; NA, Neuraminidase; pM, Picomolar.

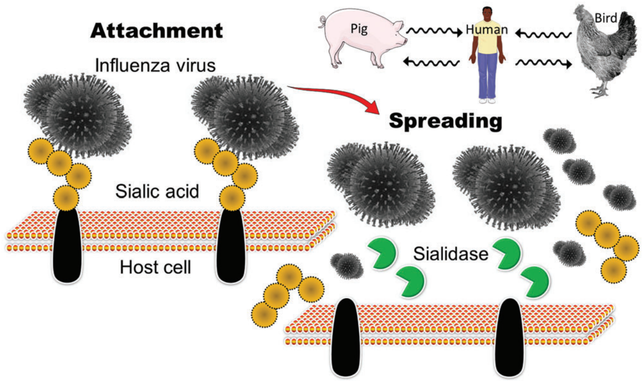

FIGURE 1 Representation of influenza virus attachment and spread. Host cell attachment by an influenza virus is shown through sialic acid. The enzyme sialidase involves detaching the virus from the host cell and infecting neighboring cells. The three major hosts circulating influenza strains are humans, pigs, and birds

and H7N7, whereas influenza B has two major lineages (Victoria and Yamagata). Among the subtypes of influenza A, swine flu (H1N1) and bird flu (H5N1) cause severe illnesses and circulate among three major hosts, namely, pigs, humans, and birds.[5]

Due to the above issues and challenges to human health and wealth, different sensing strategies have been generated for influenza virus determination and discrimination.[6–10] With the developed sensing systems, a surface antigen has been desired, aimed at detecting intact cells.[1,2] There are two predominant antigens on the surface of influenza viruses, namely, hemagglutinin (HA) and sialidase/neuraminidase (NA); HA contributes approximately 80%.[5] HA primarily attaches to the cell surface through glycans (sialic acids), whereas NA releases the virus from the host cell surface after infection (Figure 1). The current analysis was performed on an interdigitated electrode (IDE) sensor using HA as the target against the predominant probes: aptamer/antibody. Furthermore, signal enhancements were attained by conjugating the probe on a gold nanoparticle. With the available data, the validation was performed by Gaussian noise channel analysis with the assistance of Internet of Things (IoT). The primary aim of this study is to set-up a remote surveillance IoT system for influenza and other emerging and reemerging viral strains.

An IoT is a powerful technology that can effectively visualize systems such as wristwatches, smart grids, garage doors, emergency alarms, smart vehicles, and home appliances from the point of a remote control.[11] Most of the electronic devices that support our life operations participate with the IoT and are controlled remotely.[12] Recently, an artificial-intelligence-based dynamic state estimation for smart energy monitoring was presented in Ref. [13] where a statistical model was not needed. However, in stability analysis, it is desirable to exhibit a correct model. From this point, the physical model generated by the Kalman filter algorithm is potentially utilized for estimations of the dynamic state.[14–17] However, the computational complexity is high compared with that of the least-mean-square algorithm. In addition, the aforementioned works suggested that the network is ideal between the biosensors and healthcare monitoring systems.

The recognized environmentally friendly remote biosensing has been shown to be a state-space model. The IoT-based wireless sensor is considered to pass the biosensing output to the centralized system, where the estimations are affected by the noisy channels. The algorithm is formulated for determining the system states over noisy communication channels for the innovative infrastructure of the IoT in a healthcare system. The role is minimized by aligning with the estimated states and makes to a new calculation of the algorithm in IoT-based smart healthcare monitoring.

2 | EXPERIMENTAL

2.1 | Model for a controlled IoT system

The suggested IoT infrastructure for onsite determination and calculation of the system state is displayed in Figure 2. As elaborated in the supplementary information, the interconnected IoT system is considered a discrete-time-invariant model with step size Δt as,

$$x\ (k+1) = \ Ax\,(k) + Bu\,(k) + n\,(k)$$

where $x \in R^n$ is the state vector, $u \in R^m$ is the input vector, $A \in R^{n\times n}$ is the system matrix, $B \in \ R^{n\times m}$ is the input matrix, and $n(k)$ is the system noise with a zero mean Gaussian distribution.[18,19] k represents a discrete-time step. Received signal at the HMS or observation information, $z(k)$, is by:

$$z\ (k) = \ Hx\,(k) + w\,(k)$$

where H is the identity matrix and $w(k)$ is the noise, which considers the zero mean Gaussian distribution with the $R(k)$ covariance matrix. The obtained modulated signal was $m(k)$. The signal obtained at the control center is as follows:

$$r\ (k) = \ m\,(k) + n\,(k)$$

where $n(k)$ is the channel noise.

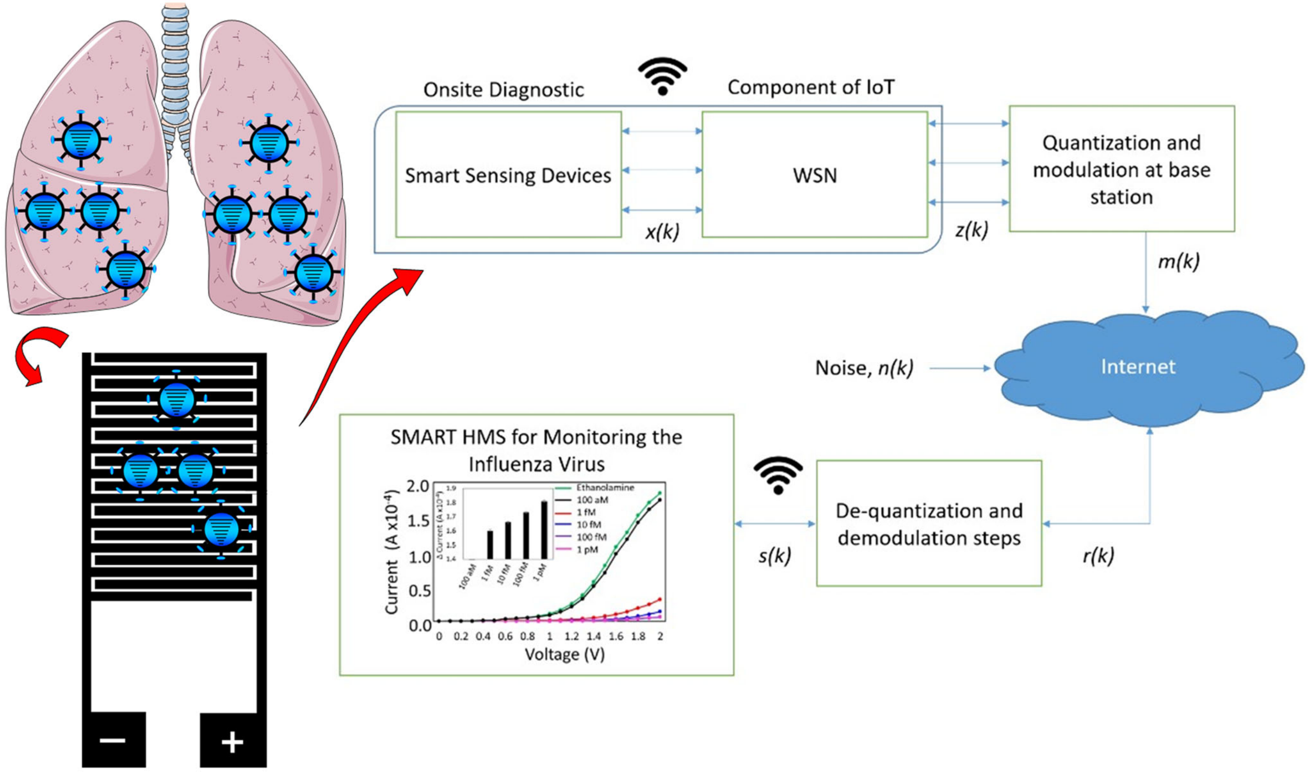

FIGURE 2 Proposed IoT architecture for the influenza surveillance system. The complete steps to apply the Gaussian noise channel are outlined. The system involves the IoT

2.2 | Designing chrome mask and fabrication

The pattern of the dielectric sensor was designed and transferred, then the fabrication process was carried out using the earlier developmental procedure.[20,21] In brief, the silicon substrate was used as a base layer and oxidized to form a silicon dioxide layer. On the silicon dioxide layer, aluminum was layered and further processed to yield above pattern designed by AutoCAD. As a result, a dielectrode pattern was created with a uniform gap and finger regions. 3D-nanoprofilometry (Hawk 3D-profilometry, USA) and high-power microscopy analyses were done to capture the clear-cut gaps between the electrodes.[22,23] The desired target(s) was determined on the chemically modified dielectrode surface assisted with the probe. It has the following steps. (i) surface modified chemically; (ii) modified probe was attached after activate the surface; (iii) the unreacted area was masked with 1 M of ethanolamine; (iv) different concentrations of the targets were added; and (v) changes in the current signal noted. Upon attaching or interacting the molecules on the gap-finger regions, there will be dipole moment happen between dual electrodes. The surface chemical/biological modifications were carried out in the presence of 10 mM PBS at the pH 7.4 to maintain the wet condition. A thorough washing was done between each modification/interaction and current–volt measurement was with conventional ammeter.

3 | RESULTS AND DISCUSSION

The fundamental of this research is to investigate required data from the patients then transferred to the cloud through the developed platform and all the information will be correlated in the mobile system and transmit the generated reports to other end. Up-dated nanotechnology on device validation and clinical phase screening using nanobiosensor overcome these issues. IDE was produced through processes of mask design and transducer fabrication. Semiconductor electrode will be designed in specific size in order to meet its behavior as a disposable chip and increase the economic and commercialization value during the manufacturing process. IoT set-up is by forming the interface between the data collection point and the delivery point. The transceiver-mediated system proposed to connect to the above-mentioned diagnostic. The data collected from the diagnostic can be amplified and passed to the transceiver then transmit to the receiving end. The receiving end has the receiver with the data interpretation software to display the acquired results digitally. This data can be compared with the past healthcare data

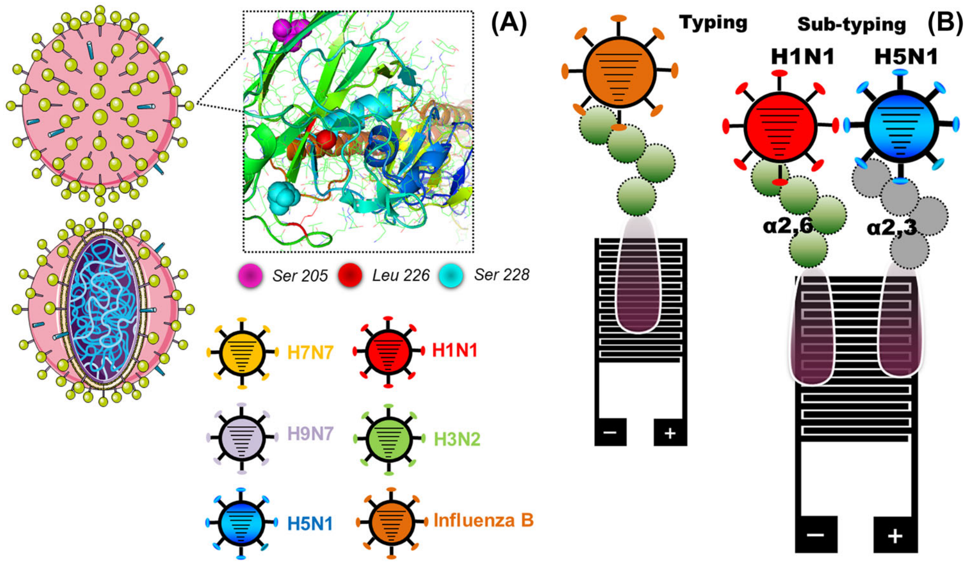

FIGURE 3 (A) Structure of influenza virus. The predominant surface antigens are hemagglutinin (HA) and neuraminidase (NA). The crystal structure (PDB Accession: 2VIU) of HA with critical amino acids for the host cell interaction is displayed. Subtypes are shown. (B) Sensing of influenza on the IDE surface. The typing and subtyping of influenza viruses are shown

of the patient and the right medicine will be prescribed. Influenza viral detection for subtyping is proposed with two major kinds of probes that have been proposed to diagnose the influenza and other infectious viruses, namely antibody and aptamer. By availing the above-described setup, with appropriate basic materials and chemical functionalization, aptamer and influenza viruses were evaluated for typing and subtyping purposes.

3.1 | Study design

This study was designed to develop a surveillance system for monitoring influenza emergence and reemergence. To accomplish this notion, the data acquired from the findings of Wang et al.[24] were correlated with a controlled IoT with Gaussian noise. The basic aim of the study was initially to determine the major surface antigen (HA) from influenza A on the dielectrode to mimic the determine of intact viruses. HA is important for attaching the influenza virus to the host cell surface by a specific sialic acid. There are two types of sialic acids, namely, α2,6 sialic acid for the human influenza interaction and α2,3 sialic acid for bird influenza; however, there are nonspecific interactions in some cases with the time of seasonal variations that occur every year.[25] For these interactions, notable amino acids, namely, serine (205), leucine (226), and serine (228), were observed (Figure 3(A)). The basic data of the interactions with HA (H1N1) were collected by an IDE sensor, which is suitable for typing and subtyping purposes (Figure 3(B)). Further insights on the closer structural views and amino acid sequences are revealed from the available sources (Figures 4(A)–4(E)).

The IDE is a dielectrode system operated using current–volt measurements by utilizing an ammeter at a linear sweep (0–2 V) with a desired step of 0.1 V (20 s) (Figure 5(A)). For the interactions with the measurements, sequential surface chemical and biological modifications were followed (Figure 5(B)). The success of the measurements is primarily due to the fabricated surface having suitable finger and gap regions for forming the proper gap and electrode sizes (10 μm). This was attested to by high-power microscopy (Figure 5(C)) and 3D-nanoprofilometry (Figure 5(D)). The gap and finger regions involve the dipole moment mechanism to transduce the signal obtained upon molecular immobilization and interaction. The variations in the current reflect the alterations in the current output. With the molecular interactions, there is an apparent difference after attaching the biomolecules (Figure 5(E)). This clear variation between the bare device and molecule-attached surface captured HA molecules by the aptamer/antibody probe. Furthermore, these two probes were conjugated with gold nanoparticles (GNPs) to enhance the performance. The data obtained with these two probes with GNPs were validated by a Gaussian noise channel-based algorithm and assisted by the IoT.

3.2 | Proposed algorithm

As elaborated in the supplementary information, given $\hat{x}(k) = A\hat{x}(k-1) + Bu(k)$ as the assumed state, with

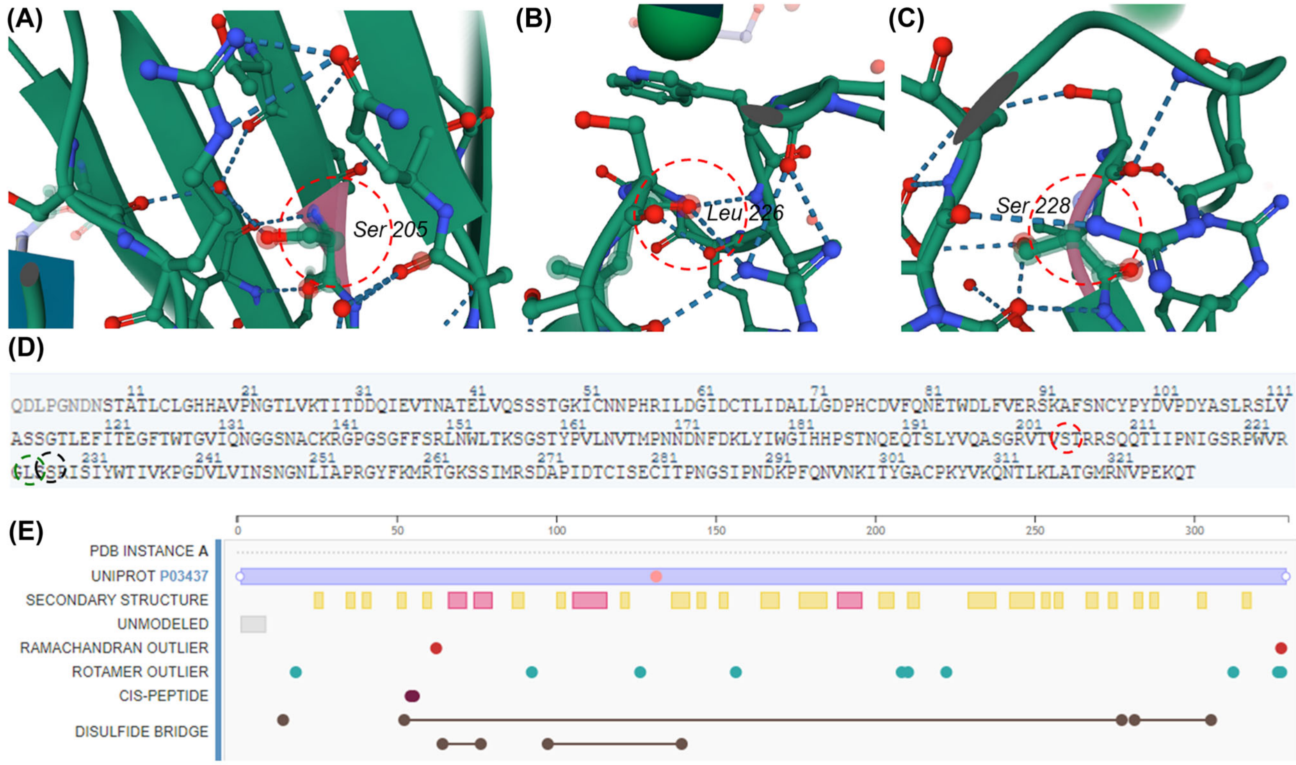

FIGURE 4 Structural information on Hemagglutinin of H1N1 influenza virus A. (A) A closer view on Ser 205; (B) a closer view on Leu 226; (C) a closer view on Ser 228. The crystal structure is from PDB Accession: 2VIU. The specific regions are as pink with a circle. (D) Amino acid sequence of hemagglutinin from H1N1. The above critical amino acids are encircled. (E) Insight on amino acid sequence of hemagglutinin from H1N1

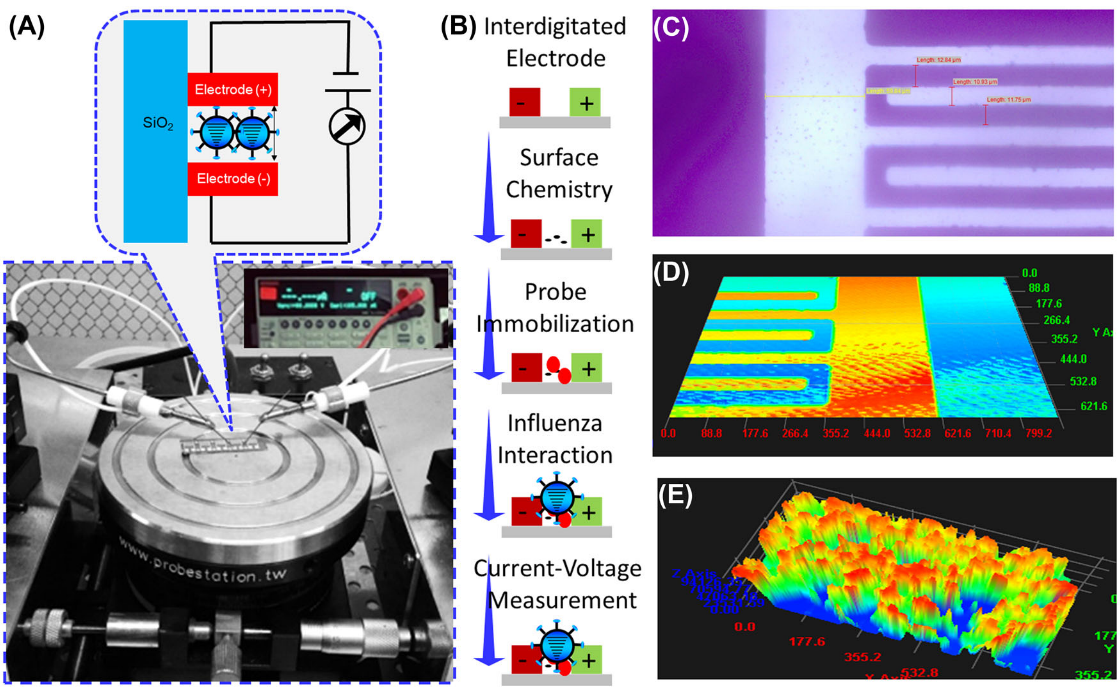

FIGURE 5 Infrastructure of the IDE. (A) Measuring system of the IDE. Current measurements (A) can be performed by the Keithley 6487 with a linear sweep of 0–2 V at a step 0.1 V (at 20 s). (B) Steps involved in the molecular attachment and measurement. Surface morphology analysis by (C) high-power microscopy; (D) 3D-profilometry on a bare IDE; and (E) 3D-profilometry after molecular attachment

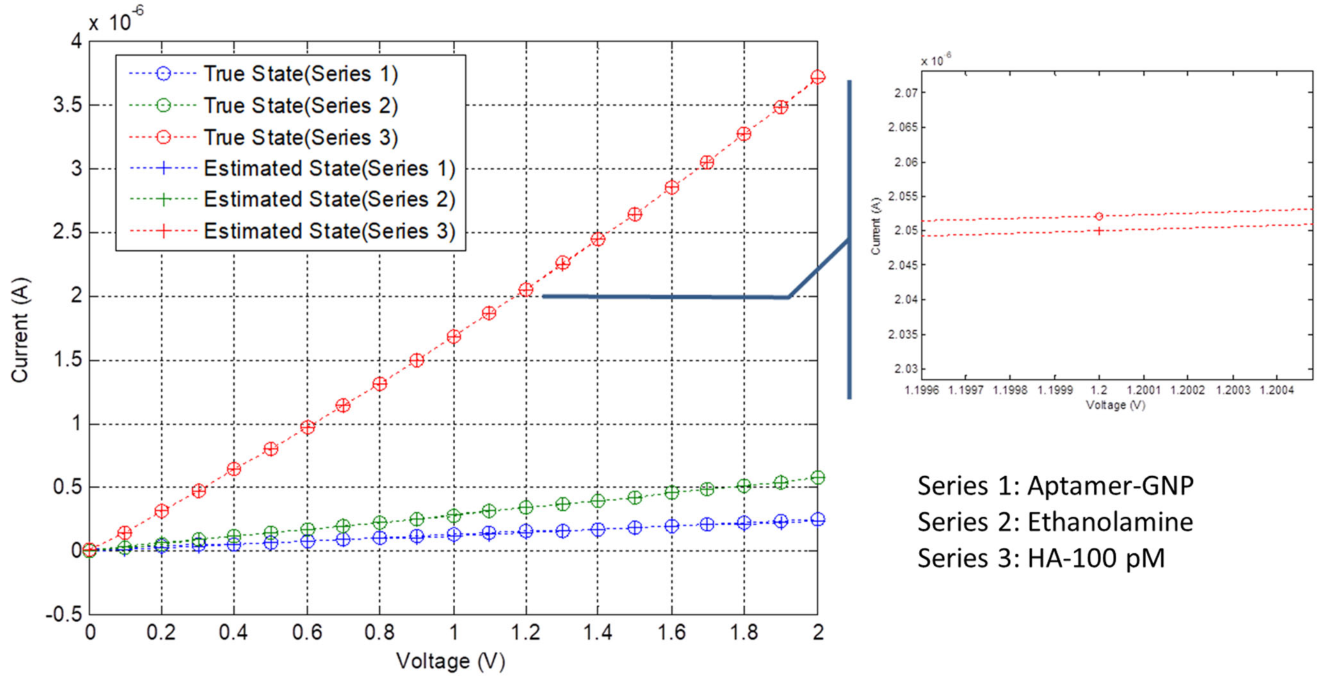

FIGURE 6 Gaussian noise channel analysis. Detection of HA by aptamer–GNP conjugates. Tested at the 100 pM level

$\hat{x}(k-1)$ being the earlier estimated state, then the state update rule can be an obtained based on the steepest descent[26]:

$$\hat{x}\ (k+1) = \hat{x}\ (k) - \mu \Delta J\,(k)$$

where μ is the scalar step size parameter, $J(k)$ is the objective function to be reduced, and $\Delta J(k)$ is the gradient descent. The cost function is

$$J\ (k) = E\left[\sum_{n=1}^{m} e_n^4\,(k)\right]$$

Here, $e_n(k)$ is the n-th error function, expressed as follows:

$$e_n\ (k) = z_n\ (k) - \hat{z}_n\,(k)$$

where $z\ (k) = H_n\ \hat{x}(k)$ and H_n is the n-th row of the observation matrix. The minimization of the cost functions is,

$$\Delta J\ (k) = \ -4\sum_{n=1}^{m} e_n^3\,(k)\,H_n^T$$

the update state determination can be expressed as:

$$\hat{x}\ (k+1) = \hat{x}\ (k) - \mu K \sum_{n=1}^{m} e_n^3\,(k)\,H_n^T$$

Here, K is the positive definite matrix, which depends on the specific application. The following normalization version is used:

$$\hat{x}\,(k+1) = \hat{x}\,(k) + \frac{\mu K \sum_{n=1}^{m} e_n^3\,(k)\,H_n^T}{\varepsilon + \|K\|_F^4}$$

ε is set as an arbitrarily small positive value to avoid division by zero. $\hat{z}(k)$ is equivalently replaced with the dequantized output $s_n(k)$, that is, $\hat{z}_n(k) \approx s_n(k)$ and the infrastructure is equivalently the reconstructed $\hat{z}_n(k)$.[27,28]

3.3 | Formal analysis

Using the above-proposed algorithmic model, the data for the interaction of HA (H1N1) against a gold nanoparticle-conjugated aptamer/antibody were validated. Figure S1 displays the data obtained with the aptamer and HA/H1N1 interaction on the ethanolamine blocked surface. These data were validated by a Gaussian noise channel-based algorithm, and there was a good correlation (Figure 6). Similarly, with the interaction of the antibody-conjugated probe and HA/H1N1, the system yielded a good correlation (Figures S2 and 7). There is no significance variation has been noticed. In general, with the sensing analysis, the variations or differences are considered if it is >10%. Furthermore, dose-dependent analysis was carried out and validated by a Gaussian noise channel-based

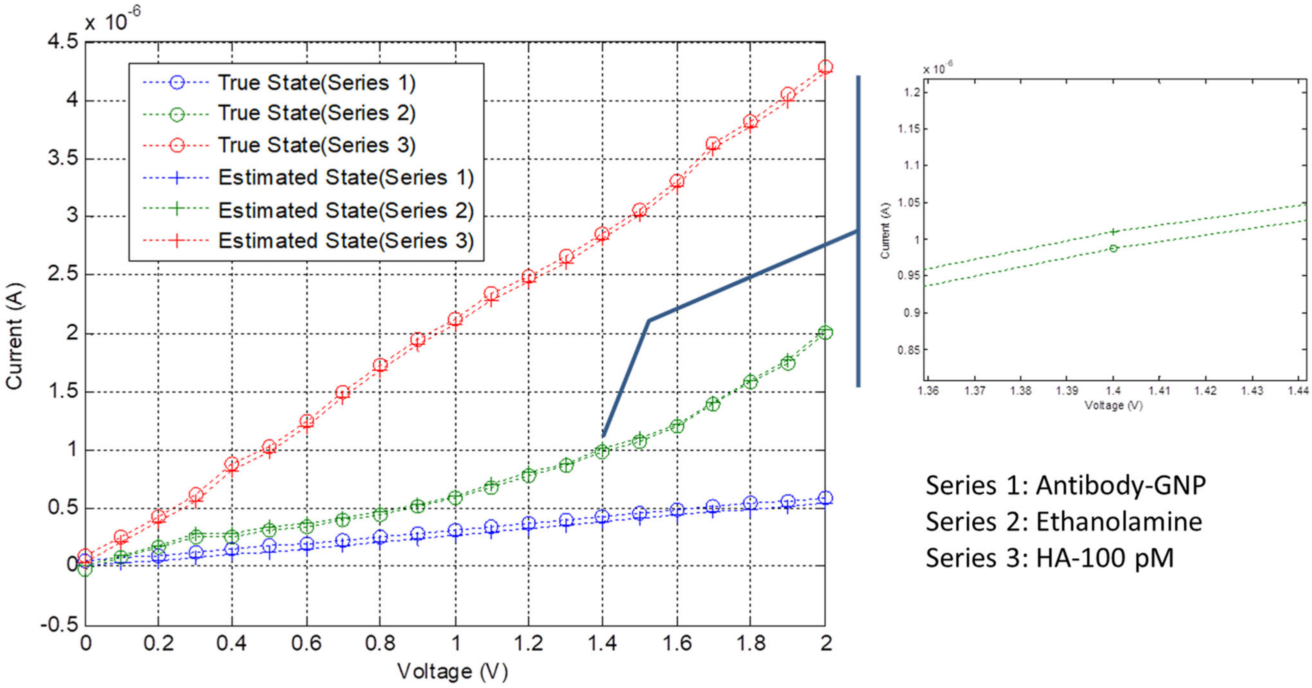

FIGURE 7 Gaussian noise channel analysis. Detection of HA by antibody–GNP conjugates. Tested at the 100 pM level

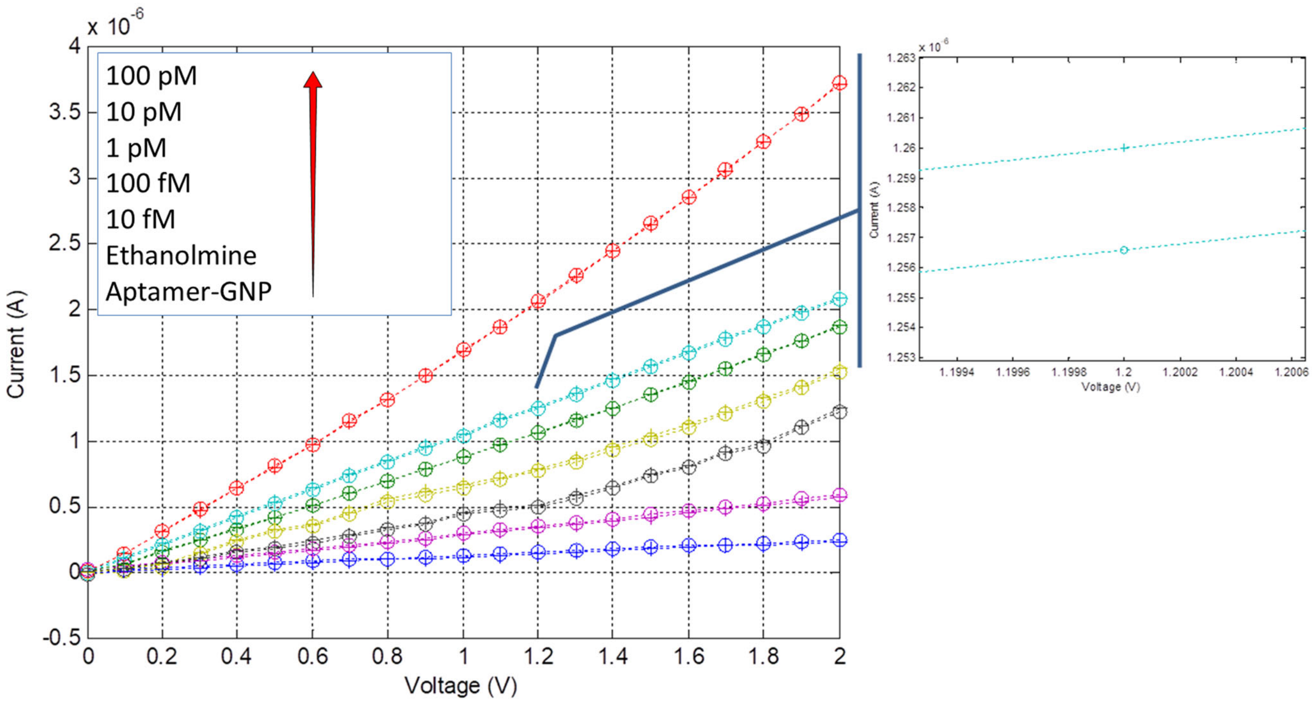

FIGURE 8 Gaussian noise channel analysis with regard to sensitivity. Detected on aptamer–GNP. HA concentrations (10 fM to 100 pM) were evaluated separately on the aptamer-immobilized surface

algorithm with aptamer–gold nanoparticles as the probe. A sharp correlation was found with increasing concentrations of HA/H1N1 against the aptamer (Figures S3 and 8). A similar response was noticed with the antibody–gold nanoparticle interaction with HA/H1N1 (Figures S4 and 9). Overall, the original data and validated data fit well and were proved by the above analyses and correlation. This model opens the way to apply some of the other algorithmic models available.[29–32] Furthermore, this kind of model development will overcome the issues with false positives.

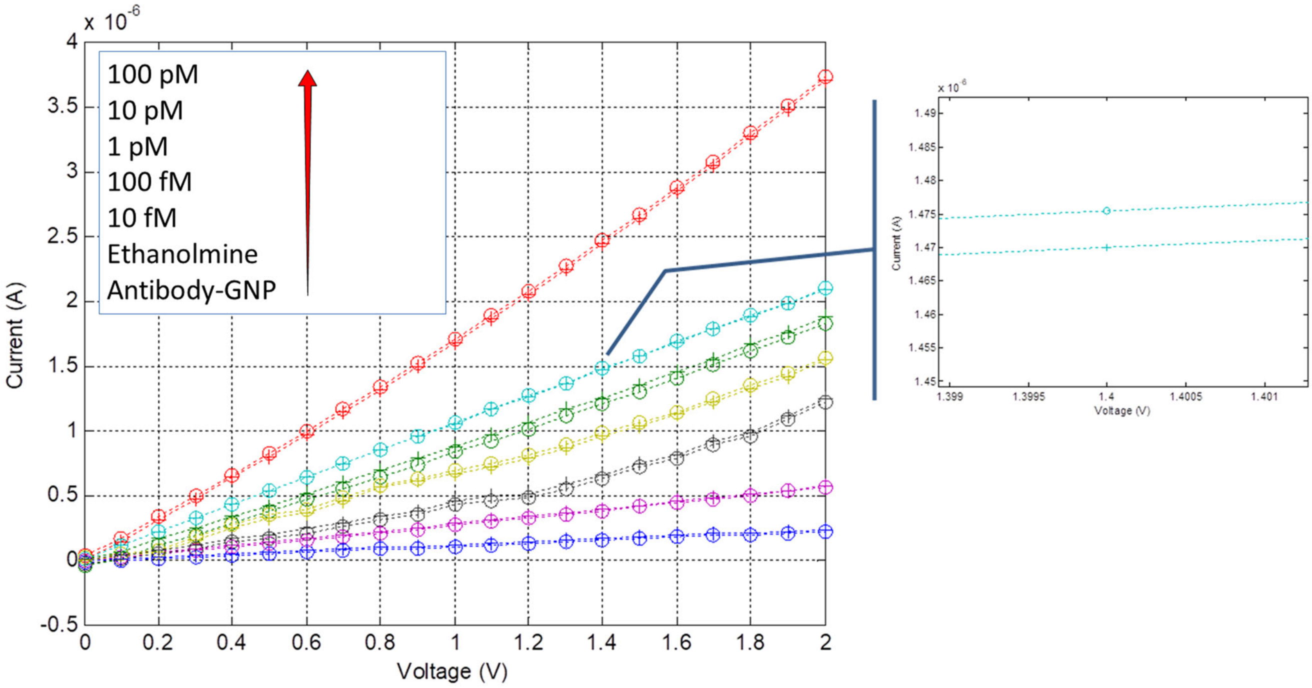

FIGURE 9 Gaussian noise channel analysis with regard to sensitivity. Detected on aptamer–GNP. HA concentrations (10 fM to 100 pM) were evaluated separately on the antibody-immobilized surface

Currently, immunochromatography testing is one of the standard methods that has been widely used. The drawback of this method is that it is able to determine the virus only after the onset of fever with a higher count of influenza viruses in the saliva sample and sometimes requires double confirmation. The current study eliminates these issues, as the IDE sensing system has several advantages over immunochromatography, including a high performance and appealing properties.

4 | CONCLUSIONS

This model study is conducted to implement a Gaussian noise channel algorithm for the surveillance of respiratory viruses during the emergence of new strains with seasonal variations. A systematic analysis was performed on the data obtained from a dielectrode (IDE) sensor with the interaction of aptamer/antibody and a surface biomarker for the influenza virus, particularly HA. HA was desired for the influenza subtype H1N1 (swine flu) and validated for digital health monitoring. The results obtained by the Gaussian noise channel algorithm fit well with the data from IDE sensing. With the combination of IDE sensing and the IoT-assisted algorithm, this strategy achieves a good alignment. This study uses H1N1 from influenza A, as it is one of the subtypes caused a severe pandemic. There are several subtypes under influenza A cause infections, which makes the importance of this study, whereas influenza B has been noticed to be comparatively infect less with only two different lineages. A proven model for the surveillance of different viruses has emerged over the past 10 decades, including the recent threat, the so-called "COVID-19," to society. This model study can be set up for precautionary surveillance to monitor viral/pathogenic spread by discriminating the subtypes in order to preserve human life and the economy. In general, with any sensing platform along with high-throughput analyses, there is a false positive due to the involvement of several samples. The current strategy is shown here to overcome this issue by proper calculations with neglecting the noticed problems in the past.

ACKNOWLEDGMENTS

This study has been supported by a grant (9001-00596) from Universiti Malaysia Perlis and a grant (R.K130000.7343.4B617) under ASEAN University Network Southeast Asia Engineering Education Development Network (AUN/Seed-Net) Special Program for Research Against COVID-19 (SPRAC).

ORCID

Subash C.B. Gopinath https://orcid.org/0000-0002-8347-4687

REFERENCES

1. Gopinath SCB Misono TS, Kawasaki K, Mizuno T, Imai M, Odagiri T, et al. An RNA aptamer that distinguishes between closely related human influenza viruses and inhibits haemagglutinin-mediated membrane fusion. J Gen Virol. 2006;87:479–87.
2. Gopinath SCB, Sakamaki Y, Kawasaki K, Kumar PKR. An efficient RNA aptamer against human influenza B virus hemagglutinin. J Biochem. 2006;139:837–46.
3. Gopinath SCB, Awazu K, Fujimaki M, Shimizu K. Evaluation of anti-A/Udorn/307/1972 antibody specificity to influenza A/H3N2 viruses using an evanescent-field coupled waveguide-mode sensor. PLoS One. 2013;8:e81396. https://doi.org/10.1371/journal.pone.0081396
4. Lakshmipriya T, Fujimaki M, Gopinath SCB, Awazu K. Generation of anti-influenza aptamers using the systematic evolution of ligands by exponential enrichment for sensing applications. Langmuir. 2013;29:15107–15.
5. Gopinath SCB, Kumar PKR. Aptamers that bind to the hemagglutinin of the recent pandemic influenza virus H1N1 and efficiently inhibit agglutination. Acta Biomater. 2013;9:8932–41. https://doi.org/10.1016/j.actbio.2013.06.016
6. Gopinath SCB, Awazu K, Fujimaki M, Shimizu K, Shima T. Observations of immuno-gold conjugates on influenza viruses using waveguide-mode sensors. PLoS One. 2013;8:1–10.
7. Park TJ et al. Imprinted microfluidic device for bioin- spired detection of avian influnza virus. Thirteenth International Conference on Miniaturized Systems for Chemistry and Life Sciences, Jeju, Korea. November 1–5, 866–868. 2009.
8. Le TT et al. Aptamer-based biosensors for the rapid visual detection of flu viruses. Chem Commun. 2014;50:15533–6.
9. Ozcelik D, Parks JW, Wall TA, Stott MA, Cai H, Parks JW, et al. Optofluidic wavelength division multiplexing for single-virus detection. Proc Natl Acad Sci USA. 2015;112:12933-7. https://doi.org/10.1073/pnas.1511921112
10. Isin B, Doruker P, Bahar I. Functional motions of influenza virus hemagglutinin: a structure-based analytical approach. Biophys J. 2002;82:569–81.
11. Lin J, Yu W, Zhang N, Yang X, Zhang H, Zhao W. A survey on internet of things: architecture, enabling technologies, security and privacy, and applications. IEEE Internet Things J. 2017;5:1125–42. https://doi.org/10.1109/JIOT.2017.2683200
12. Marjani M, Nasaruddin F, Gani A, Karim A, Hashem IAT, Siddiqa A, et al. Big IoT data analytics: architecture, opportunities, and open research challenges. IEEE Access 2017;5:5247–61. https://doi.org/10.1109/ACCESS.2017.2689040
13. Bhatia M, Sood SK. A comprehensive health assessment framework to facilitate IoT-assisted smart workouts: a predictive healthcare perspective. Comput Ind. 2017;92–93:50–66.
14. Görs M, Schäfer M, Albert M, Marx R, Schilling K. Link analysis for Networked Control Systems over mobile and wireless communication networks in telehealth. in IFAC Proceedings Volumes (IFAC-PapersOnline). 2012;45: 1–6.
15. Hostettler R, Kaltiokallio O, Yigitlery H, Särkkä S, Jänttiy R RSS-based respiratory rate monitoring using periodic Gaussian processes and Kalman filtering. in *25th European Signal Processing Conference, EUSIPCO 2017*, Janua, 2017;256–60.
16. Villeneuve E, Harwin W, Holderbaum W, Janko B, Sherratt RS. Reconstruction of angular kinematics from wrist-worn inertial sensor data for smart home healthcare. IEEE Access. 2017;5:2351–63.
17. Zhang Z, Yu Q, Zhang Q, Ning N, Li J. A Kalman filtering based adaptive threshold algorithm for QRS complex detection. Biomed Signal Process Control. 2020;58:101827.
18. Ghahremani E, Kamwa I. Online state estimation of a synchronous generator using unscented Kalman filter from phasor measurements units. IEEE Trans Energy Convers. 2011;26:1099–108.
19. Ariff MAM, Pal BC, Singh AK. Estimating dynamic model parameters for adaptive protection and control in power system. IEEE Trans Power Syst. 2015;30:829–39.
20. Bao X, Huo G, Li L, Cao X, Liu Y, Lakshmipriya T, et al. Coordinated dispersion and aggregation of gold nanorod in aptamer-mediated gestational hypertension analysis. J. Anal. Methods Chem. 2019;2019:5676159.
21. Ramanathan S et al. Assorted micro-scale interdigitated aluminium electrode fabrication for insensitive electrolyte evaluation: zeolite nanoparticle-mediated micro- to nano-scaled electrodes. Appl Phys A. 2019;125:548.
22. Letchumanan I, Gopinath SCB, Md Arshad MK, Anbu P, Lakshmipriya T. Gold nano-urchin integrated label-free amperometric aptasensing human blood clotting factor IX: a prognosticative approach for “Royal disease.. Biosens Bioelectron. 2019;131:128–35.
23. Letchumanan I, Arshad M, M K, Balakrishnan SR, Gopinath SCB. Gold-nanorod enhances dielectric voltammetry detection of c-reactive protein: a predictive strategy for cardiac failure. Biosens Bioelectron. 2019;130:40–47.
24. Wang F, Gopinath SCB, Lakshmipriya T. Aptamer-antibody complementation on multiwalled carbon nanotube-gold transduced dielectrode surfaces to detect pandemic swine influenza virus. Int. J. Nanomed. 2019;14:8469–81. https://doi.org/10.2147/IJN.S219976
25. Gopinath SCB, Awazu K, Fujimaki M, Shimizu K. Neu5Acα2,6Gal and Neu5Acα2,3Gal receptor specificities on influenza viruses determined by a waveguide-mode sensor. Acta Biomater. 2013;9:5080–7.
26. Malik MB, Salman M. State-space least mean square. Digit. Signal Process. A Rev. J. 2008;18:334–45.
27. Moosavi SR, Gia TN, Nigussie E, Rahmani AM, Virtanen S, Tenhunen H, et al. End-to-end security scheme for mobility enabled healthcare Internet of Things. Futur. Gener. Comput. Syst. 2016;64:108–24.
28. El Kafhali S, Salah K. Performance modelling and analysis of Internet of Things enabled healthcare monitoring systems. IET Networks. 2019;8:48–58.
29. Howard A, Matarić MJ, Sukhatme GS. An incremental self-deployment algorithm for mobile sensor networks. Auton. Robots. 2002;13:113–26. https://doi.org/10.1023/A:1019625207705
30. Zou Y, Chakrabarty K. Sensor deployment and target localization in distributed sensor networks. ACM Trans. Embed. Comput. Syst. 2004;3:61–91. https://doi.org/10.1145/972627.972631
31. Solari F, Shanahan JF, Ferguson RB, Adamchuk VI. An active sensor algorithm for corn nitrogen recommendations based on a chlorophyll meter algorithm. Agron J. 2010;102:1090–8. https://doi.org/10.2134/agronj2010.0009

32. Cohen O, Edan Y. A sensor fusion framework for online sensor and algorithm selection. Rob Auton Syst. 2008;56:762–76. https://doi.org/10.1016/j.robot.2007.12.002

SUPPORTING INFORMATION

Additional supporting information may be found in the online version of the article at the publisher's website.

How to cite this article: Gopinath SCB, Ismail ZH, Sekiguchi K. Biosensing epidemic and pandemic respiratory viruses: Internet of Things with Gaussian noise channel algorithmic model. Biotechnol Appl Biochem. 2022;1–10. https://doi.org/10.1002/bab.2300